Journal of Biomolecular NMR, 10 (1997) 301–306
KLUWER/ESCOM

J-Bio NMR 495

Measurement of ^{15}N-^{1}H coupling constants in uniformly ^{15}N-labeled proteins: Application to the photoactive yellow protein

Petra Düx, Brian Whitehead, Rolf Boelens, Robert Kaptein and Geerten W. Vuister*

Department of NMR Spectroscopy, Bijvoet Center for Biomolecular Research, Utrecht University, Padualaan 8, 3584 CH Utrecht, The Netherlands

Received 23 June 1997
Accepted 2 September 1997

Keywords: J-couplings; HNHB; HNHA; Quantitative J-correlation; $^{3}J(NH^{\beta})$; $^{3}J(NH^{\alpha(i-1)})$; Stereospecific assignment; Glycine residues; Photoactive yellow protein

Summary

A modified HNHB experiment is presented that allows the determination of J(NH) coupling constants directly from the ratio of cross-peak to diagonal-peak intensities. The experiment was applied to the photoactive yellow protein (PYP) and yielded the magnitude of 117 $^{3}J(NH^{\beta})$ coupling constants. In addition, 29 $^{3}J(NH^{\alpha(i-1)})$ coupling constants could be measured, providing information about the backbone angle ψ. These data, in conjunction with the magnitudes of the $^{3}J(H^{N}H^{\alpha})$ coupling constants obtained from the HNHA spectrum, effectively discriminate the two possibilities for the stereospecific assignment of the H^{α} resonances in glycine residues. For all eight glycine residues in PYP that were not subject to conformational averaging and had non-degenerate H^{α} resonance frequencies, the J-coupling data, together with limited NOE data, yielded the stereospecific assignment of the H^{α} resonances for these residues. In addition, reliable and precise ϕ,ψ dihedral constraints were also derived for these residues from the J-coupling data.

Measurement of homo- and heteronuclear J-coupling constants has been a topic of considerable interest during the last decade. The advent of isotope labeling has allowed the development of a large array of pulse sequences for measuring J-couplings which are applicable to small- and medium-sized proteins. These experiments can be divided into two main categories; the so-called E.COSY-based methods (Griesinger et al., 1986; Montelione et al., 1989; Wider et al., 1989; Gemmecker and Fesik, 1991; Emerson and Montelione, 1992; Griesinger and Eggenberger, 1992; Xu et al., 1992; Seip et al., 1994; Weisemann et al., 1994; Wang and Bax, 1995) and the quantitative J-correlation methods (Archer et al., 1991; Vuister and Bax, 1993a; Bax et al., 1994). In the E.COSY approach, the J-coupling between spins A and X in an AMX spin system is measured from the relative displacement of the multiplet components of the AM cross peak under the condition that the X spin state has not been changed when establishing the AM correlation. The alternative quantitative J-correlation method is based on quantification of the in-phase and antiphase components resulting from evolution of the J-coupling.

The $^{3}J(NH^{\beta})$ coupling constants are very useful in establishing the χ_1 rotameric state and aid the stereospecific assignment of prochiral β-methylene groups (Bystrov, 1976; Xu et al., 1992; Karimi-Nejad et al., 1994). The $^{3}J(NH^{\beta})$ coupling constant can be measured from the E.COSY pattern in a 3D ^{15}N-separated NOESY-HSQC in which the protons are not decoupled from the ^{15}N nucleus during the ^{1}H indirect evolution and acquisition dimensions (Montelione et al., 1989; Wider et al., 1989). The HNHB experiment (Archer et al., 1991; Madsen et al., 1993) employs the quantitative J-correlation method for measuring the $^{3}J(NH^{\beta})$ coupling constant. The size of the cross peak at the H^{β} frequency in the indirect proton dimension reflects the magnitude of the $^{3}J(NH^{\beta})$ coupling. For quantification, however, a separate 2D reference experiment needs to be recorded (Bax et al., 1994). The manipulation of two different spectra, which are of different dimensionality, makes this procedure somewhat cum-

*To whom correspondence should be addressed at: SON Research Center, Laboratory of Biophysical Chemistry, University of Nijmegen, Toernooiveld, 6225 ED Nijmegen, The Netherlands.

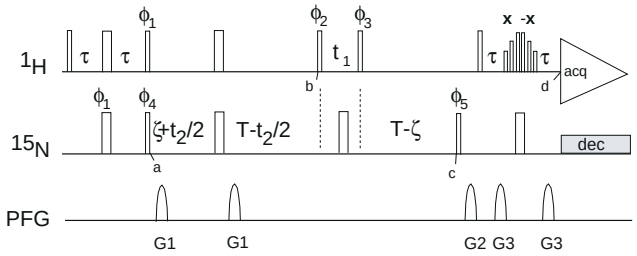

Fig. 1. Pulse sequence for the modified HNHB experiment. Narrow and wide bars denote pulses with a 90° and 180° flip angle, respectively. The 180° pulse in the final reverse INEPT was implemented as a 3α-τ-9α-τ-19α-τ-19α-τ-9α-3α WATERGATE sequence (Sklenar et al., 1993), with 26α = 180°. The phases are as follows: ϕ_1 = y,–y; ϕ_2 = 2x, 2(–x); ϕ_3 = 4x,4(–x); ϕ_4 = 4x,4(–x); ϕ_5 = 8x,8(–x); receiver = 2(x,–x,–x,x), 2(–x,x,x,–x). Pulsed-field gradients (PFG) had a sine-bell shape and were applied along the z-axis. Durations and strengths of the gradients were as follows: G_1 = 1 ms, –7 G/cm, G_2 = 1 ms, –20 G/cm, G_3 = 1 ms, 30 G/cm. The delays were as follows: τ = 2.5 ms; T = 31.9 ms; ζ = 2.66 ms. ^{15}N decoupling during acquisition was accomplished using the WALTZ-16 decoupling scheme (Shaka et al., 1983) with an rf field strength of 1.25 kHz.

bersome. Here, we present a modified HNHB experiment that allows direct extraction of the magnitude of the coupling constant from a single spectrum.

The ^{3}J(NH$^\alpha$) presents another useful coupling constant, providing information about the backbone angle ψ (Bystrov, 1976; Wang and Bax, 1995). The ^{3}J(NH$^\alpha$) coupling constant has been measured from E.COSY type experiments on uniformly ^{15}N/^{13}C-labeled proteins (Seip et al., 1994; Weisemann et al., 1994; Wang and Bax, 1995). However, information about the magnitude of the ^{3}J(NH$^\alpha$) coupling is also contained in the E.COSY and HNHB experiments mentioned above for measuring ^{3}J(NH$^\beta$). We will show that accurate values of ^{3}J(NH$^\alpha$) can often be obtained from the HNHB experiment. In particular for glycine residues, this knowledge of ^{3}J(NH$^\alpha$), in conjunction with knowledge of ^{3}J(H^{N}H$^\alpha$) obtained from the HNHA experiment (Vuister and Bax, 1993a), greatly aids the stereospecific assignment of the diastereotopic α-protons and yields ϕ,ψ dihedral angle constraints.

The pulse sequence used in the present study for measuring the 3D HNHB spectrum is shown in Fig. 1. The original sequence (Archer et al., 1991; Madsen et al., 1993) is modified to allow quantitative measurement of the J-coupling from one experiment. This was accomplished by changing the dephasing and rephasing periods, as discussed below.

At time point *a* in the sequence antiphase ^{15}N magnetization, $2\mathbf{N}_y\mathbf{H}^N_z$, has been created where $\mathbf{H}^N$ and $\mathbf{N}$ denote the ^{1}H^N and ^{15}N spin operators of the product-operator formalism (Sørensen et al., 1983), respectively. The antiphase ^{15}N magnetization will evolve under the influence of the ^{15}N chemical shift and the ^{1}J(NH), ^{3}J(NH$^\alpha$), and ^{3}J(NH$^\beta$) couplings. Temporarily neglecting the ^{15}N chemical shift, and considering first only the effects of ^{1}J(NH) and one of the ^{3}J(NH) coupling constants, the magnetization at time point *b* has evolved to:

$$\begin{aligned} &2\mathbf{N}_y\mathbf{H}^N_z \xrightarrow{T+\zeta} \\ &2\mathbf{N}_y\mathbf{H}^N_z \cos(\pi\,{}^1J_{NH}[T+\zeta])\cos(\pi\,{}^3J_{NHi}[T+\zeta]) \\ &-4\mathbf{N}_x\mathbf{H}^N_z\mathbf{H}^i_z \cos(\pi\,{}^1J_{NH}[T+\zeta])\sin(\pi\,{}^3J_{NHi}[T+\zeta]) \\ &-\mathbf{N}_x \sin(\pi\,{}^1J_{NH}[T+\zeta])\cos(\pi\,{}^3J_{NHi}[T+\zeta]) \\ &-2\mathbf{N}_y\mathbf{H}^i_z \sin(\pi\,{}^1J_{NH}[T+\zeta])\sin(\pi\,{}^3J_{NHi}[T+\zeta]) \end{aligned} \quad (1)$$

where $\mathbf{H}^i$ denotes a proton spin operator, other than the $\mathbf{H}^N$, which has a three-bond coupling, $^3J_{NHi}$, with the $\mathbf{N}$ operator, and $^1J_{NH}$ denotes the one-bond ^{15}N-H^N J-coupling. The 90°(ϕ_2) proton pulse selects for the $2\mathbf{N}_y\mathbf{H}^N_z$ and $2\mathbf{N}_y\mathbf{H}^i_z$ operators and converts these terms into heteronuclear multiple-quantum operators, which evolve during t_1 as pseudo single-quantum with the H^N and H^i frequencies, respectively. Temporarily omitting the trigonometric factors from Eq. 1, we obtain

$$\begin{aligned} &(1) \xrightarrow{90°(\phi_2)} \xrightarrow{t_1} \\ &-2\mathbf{N}_y\mathbf{H}^N_y \cos(\omega_{HN}t_1) + 2\mathbf{N}_y\mathbf{H}^N_x \sin(\omega_{HN}t_1) \\ &+2\mathbf{N}_y\mathbf{H}^i_y \cos(\omega_{Hi}t_1) - 2\mathbf{N}_y\mathbf{H}^i_x \sin(\omega_{Hi}t_1) \end{aligned} \quad (2)$$

As was the case in the original HNHB pulse scheme, the proton 90°(ϕ_3) selects the $\mathbf{H}_y$-containing operators and converts the magnetization back into ^{15}N antiphase terms, which refocus during the subsequent delay of T–ζ under the influence of the ^{1}J(NH), ^{3}J(NH$^\alpha$), and ^{3}J(NH$^\beta$) couplings. At time point *c* the following operators exist, after reintroducing the previously omitted trigonometric factors

$$\begin{aligned} &(2) \xrightarrow{90°(\phi_3)} \xrightarrow{T-\zeta} \\ &-\{2\mathbf{N}_y\mathbf{H}^N_z \cos(\pi\,{}^1J_{NH}[T-\zeta])\cos(\pi\,{}^3J_{NHi}[T-\zeta]) \\ &\quad -4\mathbf{N}_x\mathbf{H}^N_z\mathbf{H}^i_z \cos(\pi\,{}^1J_{NH}[T-\zeta])\sin(\pi\,{}^3J_{NHi}[T-\zeta]) \\ &\quad -\mathbf{N}_x \sin(\pi\,{}^1J_{NH}[T-\zeta])\cos(\pi\,{}^3J_{NHi}[T-\zeta]) \\ &\quad -2\mathbf{N}_y\mathbf{H}^i_z \sin(\pi\,{}^1J_{NH}[T-\zeta])\sin(\pi\,{}^3J_{NHi}[T-\zeta])\} \\ &\times \cos(\pi\,{}^1J_{NH}[T+\zeta])\cos(\pi\,{}^3J_{NHi}[T+\zeta])\cos(\omega_{HN}t_1) \\ &+\{2\mathbf{N}_y\mathbf{H}^i_z \cos(\pi\,{}^1J_{NH}[T-\zeta])\cos(\pi\,{}^3J_{NHi}[T-\zeta]) \\ &\quad -\mathbf{N}_x \cos(\pi\,{}^1J_{NH}[T-\zeta])\sin(\pi\,{}^3J_{NHi}[T-\zeta]) \\ &\quad -4\mathbf{N}_x\mathbf{H}^N_z\mathbf{H}^i_z \sin(\pi\,{}^1J_{NH}[T-\zeta])\cos(\pi\,{}^3J_{NHi}[T-\zeta]) \\ &\quad -2\mathbf{N}_y\mathbf{H}^N_z \sin(\pi\,{}^1J_{NH}[T-\zeta])\sin(\pi\,{}^3J_{NHi}[T-\zeta])\} \\ &\times \sin(\pi\,{}^1J_{NH}[T+\zeta])\sin(\pi\,{}^3J_{NHi}[T+\zeta])\cos(\omega_{Hi}t_1) \end{aligned} \quad (3)$$

Only the $2\mathbf{N}_y\mathbf{H}^N_z$ operators are transferred to observable amide proton magnetization by the reverse INEPT scheme with a WATERGATE 180° proton pulse. At time point *d*, just prior to detection, the following term exists

$$\begin{aligned} &(3) \xrightarrow{\text{rev-INEPT}} \\ &-\mathbf{H}^N_x \{\cos(\pi\,{}^1J_{NH}[T-\zeta])\cos(\pi\,{}^3J_{NHi}[T-\zeta]) \\ &\quad \times \cos(\pi\,{}^1J_{NH}[T+\zeta])\cos(\pi\,{}^3J_{NHi}[T+\zeta])\cos(\omega_{HN}t_1) \\ &\quad +\sin(\pi\,{}^1J_{NH}[T+\zeta])\sin(\pi\,{}^3J_{NHi}[T+\zeta]) \\ &\quad \times \sin(\pi\,{}^1J_{NH}[T-\zeta])\sin(\pi\,{}^3J_{NHi}[T-\zeta])\cos(\omega_{Hi}t_1)\} \end{aligned} \quad (4)$$

Equation 4 shows that the final detected magnetization contains terms modulating with the H^i frequency in t_1 pro-

portional to $\sin(\pi\,^1J_{NH}[T+\zeta])\sin(\pi\,^3J_{NHi}[T+\zeta])\sin(\pi\,^1J_{NH}[T-\zeta])\sin(\pi\,^3J_{NHi}[T-\zeta])$ and a so-called 'diagonal' term modulating in t_1 with the H^N frequency proportional to $\cos(\pi\,^1J_{NH}[T+\zeta])\cos(\pi\,^3J_{NHi}[T+\zeta])\cos(\pi\,^1J_{NH}[T-\zeta])\cos(\pi\,^3J_{NHi}[T-\zeta])$. Provided $^1J_{NH}$ is known, $^3J_{NHi}$ can be calculated in a straightforward fashion from the ratio of the volumes of the two cross peaks along the F1 axis.

The original HNHB experiment is obtained by setting $\zeta = 0$ and $T = n/(2 \times {}^1J_{NH})$ with $n = 1,3,5,\ldots$. Clearly, Eq. 4 shows that for these settings the intensity of the diagonal peak vanishes. Quantitative extraction of the ^3J values then requires recording a separate two-dimensional reference experiment (Bax et al., 1994) selecting for the $\mathbf{N}_x$ operator (the third term of Eq. 1).

The amide $^1J_{NH}$ coupling constant in proteins varies less than 2 Hz around its average value of 94 Hz (Tolman et al., 1995; Tjandra et al., 1996). Potentially, this knowledge could be used to obtain a 'diagonal' peak of known intensity in the 3D spectrum which then can be used for extraction of the ^3J value directly from the 3D spectrum. Setting $\zeta = 0$ and $T = n/(4 \times {}^1J_{NH})$ with $n = 1,3,5,\ldots$ would result in $|\sin(\pi\,^1J_{NH}T)| = |\cos(\pi\,^1J_{NH}T)|$ and hence the cross-peak to diagonal-peak ratio would directly yield the $^3J_{NHi}$ coupling constant. The small value of $^3J_{NHi}$ requires substantial dephasing and rephasing delays; typically T is in the 30–40 ms range. However, because of these long delays, small differences in the $^1J_{NH}$ values would result in unacceptable errors in the calculated coupling constants. This is illustrated in Fig. 2, where $\tan^2(\pi\,^1J_{NH}T)$ values are plotted as a function of $^1J_{NH}$ for T = 29.3 ms (n=11) and T = 34.6 ms (n=13). Figure 2 shows that for T = 29.3 ms and for $^1J_{NH}$ values of 92 and 96 Hz the errors are already as large as 115% and 54%, respectively, whereas for T = 34.6 ms the errors are 60% and 150%, respectively.

Setting $\zeta = 1/(4 \times {}^1J_{NH})$ and $T = n/{}^1J_{NH}$ with $n = 1,2,3,\ldots$ yields much better results, as the errors in dephasing and rephasing counteract each other. The resulting curve of $\tan(\pi\,^1J_{NH}[T+\zeta])\tan(\pi\,^1J_{NH}[T-\zeta])$ for T = 31.9 ms (n=3) is also shown in Fig. 2. Clearly, the value is almost −1 for $^1J_{NH}$ in the range 92–96 Hz, the error being less than 2%. Consequently, using this scheme the cross-peak to diagonal-peak ratio, I^{cross}/I^{diag}, can be directly used for extraction of the $^3J_{NHi}$ value:

$$\begin{aligned} I^{cross}/I^{diag} &= -\tan(\pi\,^3J_{NHi}[T+\zeta])\,\tan(\pi\,^3J_{NHi}[T-\zeta]) \\ &\approx -\tan^2(\pi\,^3J_{NHi}T) \end{aligned} \qquad (5)$$

if $\zeta \ll T$. Calculations using T = 31.9 ms, ζ = 2.66 ms, a $^3J_{NHi}$ value of 8 Hz, and a $^1J_{NH}$ variation of ±2 Hz show that the total error resulting from Eq. 5 is less than 3%, and therefore the method can be expected to yield reliable results.

Relative to the original version of the HNHB experiment, the present method attenuates the cross peak by a factor $\sin(\pi\,^1J_{NH}[T+\zeta])\sin(\pi\,^1J_{NH}[T-\zeta])$, which equals −0.5 for the above settings of T and ζ. Note, however, that by increasing ζ the cross-peak signal is increased at the expense of the diagonal-peak signal. In principle, this is the desirable situation as the cross peaks tend to be smaller when compared to the diagonal peaks. By setting ζ = 4 ms the $\sin(\pi\,^1J_{NH}[T+\zeta])\sin(\pi\,^1J_{NH}[T-\zeta])$ term equals −0.86, thus considerably improving the sensitivity. However, the effect of varying values of $^1J_{NH}$ becomes more pronounced as the cancellation of errors becomes less efficient. For ζ = 4 ms the error equals ±16% for ±2 Hz variation in $^1J_{NH}$. Thus, the choice of ζ = 2.7 ms presents a good compromise, yielding small errors due to the variation in $^1J_{NH}$ and a simple scaling ratio, i.e. −1, resulting from the $\tan(\pi\,^1J_{NH}[T+\zeta])\tan(\pi\,^1J_{NH}[T-\zeta])$ term at an acceptable cost in sensitivity.

Chemical shift labeling with the ^{15}N frequency is accomplished by changing the 180°(H,N) pulses in a constant time fashion, as proposed by Madsen et al. (1993). The effect on the operators is straightforward and will not be discussed here.

The NMR experiments were recorded at 311 K on a 2 mM solution of uniformly ^{15}N-labeled photoactive yellow protein (PYP) in 95/5 (v/v) H_2O/D_2O solution at pH 5.8. The HNHB experiment was recorded using the pulse sequence of Fig. 1 on a Varian UnityPlus spectrometer equipped with a triple-resonance probe with a shielded z-gradient coil and operating at 499.91 MHz ^1H resonance frequency. The spectrum consisted of 47 (t_1,^1H) × 96 (t_2, ^{15}N) × 512 (t_3,^1H) complex points with maximum acquisition times of 9.6 (t_1), 60.1 (t_2) and 76.8 (t_3) ms. The HNHA spectrum was recorded with a pulse sequence described before (Vuister and Bax, 1993a), using a Bruker AMX2 spectrometer which was also equipped with a triple-resonance probe with a shielded z-gradient coil, and operating at 600.13 MHz ^1H resonance frequency. The spectrum

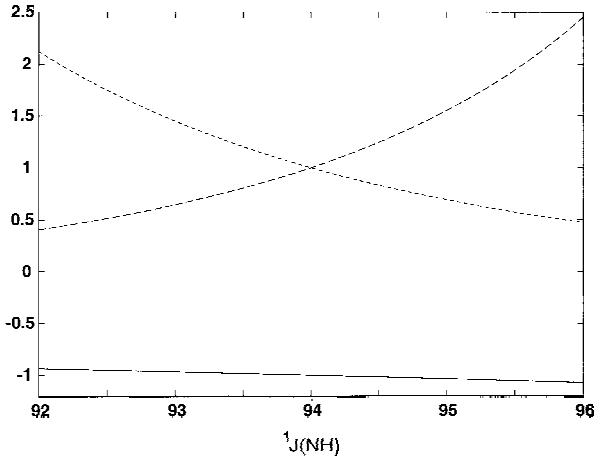

Fig. 2. Effect of variation of $^1J_{HN}$ on the determination of the coupling constant. Plotted are $\tan^2(\pi\,^1J_{HN}T)$ with T = 29.3 ms (small dashes), $\tan^2(\pi\,^1J_{HN}T)$ with T = 34.6 ms (large dashes), and $\tan[\pi\,^1J_{HN}(T-\zeta)]\tan[\pi\,^1J_{HN}(T+\zeta)]$ with T = 31.9 ms and ζ = 2.66 ms (solid line). Refer to the text for further details.

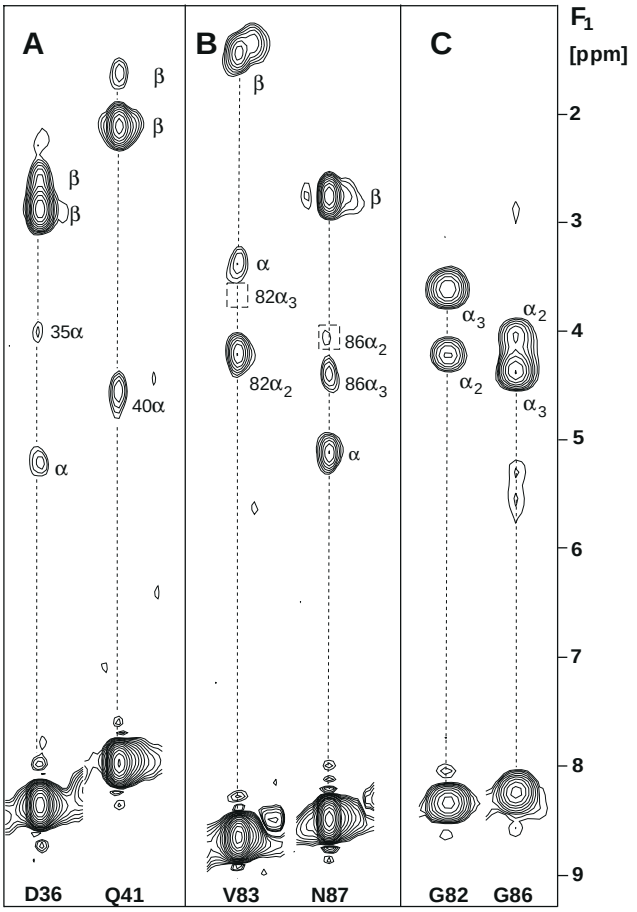

Fig. 3. Strips from the HNHB (A,B) and HNHA (C) spectra of PYP, taken at the (F2,F3) = (^{15}N,^{1}H^{N}) resonance frequencies of residues (A) Asp[36] and Gln[41], (B) Val[83] and Asn[87], and (C) Gly[82] and Gly[86]. 'Diagonal' peaks between 7–9 ppm are of opposite sign compared to 'cross' peaks. Correlations to intraresidual H$^{\alpha}$ and H$^{\beta}$ are labeled 'α' and 'β', respectively, whereas correlations to the sequential H$^{\alpha}$ are denoted by 'residue number + α'.

consisted of 50 (t_1,^{1}H) × 59 (t_2,^{15}N) × 512 (t_3,^{1}H) complex points with maximum acquisition times of 11.6 (t_1), 26.5 (t_2) and 51.3 (t_3) ms. All data were processed using NMRPipe (Delaglio et al., 1995) and analysed using the REGINE software package (Kleywegt et al., 1993). Peak positions and intensities were determined using automatic parabolic interpolation in all three dimensions of local peak maxima. ^{3}J values derived from cross-peak to diagonal-peak ratios were corrected for the faster relaxation of the antiphase magnetization, as described before (Vuister and Bax, 1993a), by multiplying all values by 1.05.

Figure 3A shows strips from the 3D HNHB spectrum of PYP taken at the (F2,F3) = (^{15}N,^{1}H^{N}) resonance frequencies of residues Asp[36] and Gln[41]. Both strips show correlations to two β-protons, the intensities of which are directly proportional to the magnitude of the ^{3}J(NH$^{\beta}$) couplings. Using Eq. 5, the ratio of cross-peak to diagonal-peak intensities yields the latter coupling constant. Assuming a negative sign for the ^{3}J(NH$^{\beta}$) couplings (Bystrov, 1976), we thus calculate values of –2.4 and –4.7 Hz for the two β-protons of Asp[36]. These values are somewhat intermediate when compared to values observed before (Bystrov, 1976; Xu et al., 1992; Karimi-Nejad et al., 1994), and could be indicative of rotameric averaging. H$^{\beta 2}$-H$^{\beta 3}$ cross-relaxation, however, will also tend to equalize the buildup of the two antiphase magnetization terms and hence decreases the intensity of the largest cross peak, with a concomitant increase in the other cross peak. The systematic errors resulting from this effect have been investigated before for the LRCH experiment. For the buildup of C$^{\delta}$H$^{\beta}$ antiphase magnetization of leucine residues in staphylococcal nuclease, it was estimated to result in an approximately 0.5 Hz systematic error for a dephasing time of 15.8 ms (Vuister et al., 1993). The present experiment employs a dephasing time of 31.9 ms, which would further increase these systematic errors. However, PYP has a rotational correlation time of 6.4 ns (Düx et al., manuscript in preparation), as compared to 9 ns for staphylococcal nuclease, yielding smaller cross-relaxation rates. Overall, for conformations in which one of the H$^{\beta}$ is *trans* with respect to the nitrogen we estimate the systematic errors resulting from this H$^{\beta 2}$-H$^{\beta 3}$ cross relaxation to be in the 0.5–1.0 Hz range. For several residues we measured values in the –5 to –6 Hz range (cf. Table 1 of the Supplementary Material), with the second J-coupling in the –1 to 0 Hz range, in accordance with a staggered rotamer (Bystrov, 1976).

In addition to ^{3}J(NH$^{\beta}$), also ^{2}J(NH$^{\alpha}$) and ^{3}J(NH$^{\alpha(i-1)}$) result in correlations in the HNHB spectrum, albeit of smaller intensity due to the generally smaller magnitudes of these J-couplings. Examples of these cross peaks are also indicated in Fig. 3A. Overall, 117 ^{3}J(NH$^{\beta}$) and 29 ^{3}J(NH$^{\alpha(i-1)}$) couplings could be extracted from the HNHB spectrum. These values are listed in Table 1 of the Supplementary Material, which can be extracted from our website http://www-nmr.chem.ruu.nl/publications-1997.html.

Stereospecific assignments of glycine H$^{\alpha}$ resonances and reliable backbone constraints are of great importance in the structure determination process, since these residues are often involved in only a limited number of NOE interactions. Thus, they can contribute significantly to the observed conformational variability of an NMR determined structure. Moreover, the glycine residues are allowed in the positive ϕ region of the Ramachandran plot and are frequently involved in turns. PYP contains 13 glycine residues out of a total of 125 amino acids, and stereospecific assignments and reliable backbone constraints are expected to be of importance to the structure determination.

Figure 3B shows the F1 strips from the 3D HNHB spectrum of PYP taken at the (F2,F3) = (^{15}N,^{1}H^{N}) resonance frequencies of residues Val[83] and Asn[87], which directly follow residues Gly[82] and Gly[86], respectively. Correla-

tions to the α-protons of the glycine residues are indicated. In both strips, a relatively large cross peak is observed for one of the glycine α-protons, corresponding to couplings of −1.9 and −1.2 Hz for Gly^{82} and Gly^{86}, respectively. The boxes indicate the resonance position of the second α-proton. The thermal noise level provides an upper limit for the coupling constants involving these protons (> −0.7 Hz in both cases). The −1.9 to −1.2 Hz values of the $^3J(NH^{\alpha(i-1)})$ observed for one of the α-protons is consistent with a *trans* conformation of this proton with respect to the sequential nitrogen nucleus (Wang and Bax, 1995). However, since there are two α-protons, two possibilities arise, e.g. $\psi \approx -60°$ or $\psi \approx +60°$. Although the $^3J(H^NH^\alpha)$ coupling constants are related to the backbone angle φ, they provide a solution, as will be discussed below.

The HNHA experiment (Vuister and Bax, 1993a) allows for the measurement of $^3J(H^NH^\alpha)$ coupling constants to both α-protons of glycine residues in a convenient way, provided that they show no overlap within the linewidth of the indirectly detected proton dimension. Strips taken from the HNHA spectrum of PYP at the (F2,F3) = (^{15}N, $^1H^N$) resonance frequencies of residues Gly^{82} and Gly^{86} are shown in Fig. 3C. Again, the coupling constants are derived from the cross-peak to diagonal-peak ratio and their values are also listed in Table 1. For Gly^{82}, values of 5.1 and 6.5 Hz are measured for $H^{\alpha 2}$ and $H^{\alpha 3}$, respectively. Using the previously parameterized Karplus curve for $^3J(H^NH^\alpha)$ (Pardi et al., 1984; Vuister and Bax, 1993a; Wang and Bax, 1996), both $\phi \approx +60°$ and $\phi \approx -60°$ yield the measured values, where each conformation is associated with one choice of the stereospecific assignment. However, the α-proton associated with $^3J(H^NH^\alpha) = 5.1$ Hz has $^3J(NH^{\alpha(i-1)}) = -1.9$ Hz. This excludes two out of the total of four possible solutions and only $\phi,\psi \approx -60°$ or $\phi,\psi \approx +60°$ are possible. Since NOE data indicate that Gly^{82} is in an α-helical conformation, the two remaining options can be discriminated. The HNHB and HNHA strips for Asn^{87} and Gly^{86} are also shown in Figs. 3B and 3C, respectively. In this case the opposite situation is encountered, with φ in the positive allowed region of the Ramachandran plot. Overall, for all eight glycine residues showing no overlap or conformational averaging, it was possible to obtain the stereospecific assignments and accurate

TABLE 1
$^3J(H^NH^\alpha)$ AND $^3J(H^\alpha N^{i+1})$ VALUES, STEREOSPECIFIC ASSIGNMENTS, AND ROTAMER RESTRAINTS FOR THE GLYCINE RESIDUES IN PYP

Residue	Shift (ppm)	$^3J(H^NH^\alpha)$ (Hz)	$^3J(H^\alpha N^{i+1})$ [a] (Hz)	Assign	Restraint[b]	
					φ	ψ
Gly^{7}	2.96	nd	> −0.8	nd		
	3.59	nd	> −0.8	nd		
Gly^{21}	4.06	5.3–7.0	−1.5 to −0.8	ov		
	4.14	5.3–7.0	−1.5 to −0.8	ov		
Gly^{25}	3.85	5.5	−1.3	$H^{\alpha 3}$	−100 < φ < −80	
	4.40	8.5	> −1.2	$H^{\alpha 2}$		20 < ψ<35 or 85 < ψ < 100
Gly^{29}	4.50	4.2–6.4	> −1.0	ov		
	4.68	4.2–6.4	> −1.0	ov		
Gly^{35}	3.99	4.0–6.1	−1.1 to 0	ov		
	3.99	4.0–6.1	−1.1 to 0	ov		
Gly^{37}	3.66	5.1	> −0.9	$H^{\alpha 2}$	80 < φ < 100	
	4.58	8.2	−1.0	$H^{\alpha 3}$		10 < ψ < 25
Gly^{47}	4.16	6.3	> −0.6	$H^{\alpha 3}$	−70 < φ < −50	
	4.41	4.0	−1.4	$H^{\alpha 2}$		−35 < ψ < −15
Gly^{51}	4.00	5.6	−1.3	$H^{\alpha 2}$	80 < φ < 100	
	4.27	6.9	ov	$H^{\alpha 3}$		−20 < ψ < −5
Gly^{59}	3.74	5.1	−1.2	$H^{\alpha 2}$	80 < φ < 100	
	4.41	7.5	ov	$H^{\alpha 3}$		−30 < ψ < −10
Gly^{77}	3.54	3.3	−2.0	$H^{\alpha 2}$	−60 < φ < −40	
	4.14	5.9	ov	$H^{\alpha 3}$		−75 < ψ < −40
Gly^{82}	3.62	6.5	> −0.7	$H^{\alpha 3}$	−70 < φ < −60	
	4.17	5.1	−1.9	$H^{\alpha 2}$		−75 < ψ < −40
Gly^{86}	4.04	5.2	> −0.7	$H^{\alpha 2}$	80 < φ < 100	
	4.36	7.3	−1.2	$H^{\alpha 3}$		15 < ψ < 30
Gly^{115}	3.73	6.0	> −0.8	nd	av	
	4.20	6.3	> −0.8	nd		av

Assign: assignment; av: averaged; nd: not determined; ov: (partial) overlap.
[a] Sign inferred from previous work (Wang and Bax, 1995).
[b] Restraint ranges were derived assuming the absence of rotamer averaging and used NOE data to exclude certain φ,ψ combinations (see text).

backbone restraints. The values are listed in Table 1. Application of these data to the structure calculation of PYP reduced the pairwise backbone rmsd from 0.83 to 0.73 Å (Düx et al., manuscript in preparation).

In conclusion, we have shown that accurate values of $^{3}J(NH^{\beta})$ and $^{3}J(NH^{\alpha(i-1)})$ can be obtained directly from a modified HNHB experiment using the ratio of two peaks along the F1 axis, hence alleviating the requirement of a $^{15}N/^{13}C$-labeled sample for measuring these coupling constants. The $^{3}J(NH^{\alpha(i-1)})$ values, in conjunction with $^{3}J(H^{N}H^{\alpha})$ values, are particularly useful for obtaining ϕ,ψ dihedral constraints and stereospecific assignment of glycine H^{α} resonances. The modification presented here for the HNHB experiment can also be applied in a similar fashion to other quantitative J-correlation experiments that require a separate reference experiment of lower dimensionality, such as the LRCH experiment (Vuister et al., 1993; Vuister and Bax, 1993b), provided a uniform coupling can be exploited to obtain the reference peak.

Acknowledgements

The authors thank Dr. Jasmin Karimi-Nejad for assistance with the HNHA experiment and Prof. Klaas J. Hellingwerf for providing the ^{15}N-labeled PYP. G.W.V. has been financially supported by the Royal Netherlands Academy of Arts and Sciences. This work was also supported by the Netherlands Foundation for Chemical Research (SON) with financial assistance from the Netherlands Organization for Scientific Research (NWO).

References

Archer, S.J., Ikura, M., Torchia, D.A. and Bax, A. (1991) *J. Magn. Reson.*, **95**, 636–641.

Bax, A., Vuister, G.W., Grzesiek, S., Delaglio, F., Wang, A.C., Tschudin, R. and Zhu, G. (1994) *Methods Enzymol.*, **239**, 79–105.

Bystrov, V.F. (1976) *Prog. NMR Spectrosc.*, **10**, 41–81.

Delaglio, F., Grzesiek, S., Vuister, G.W., Zhu, G., Pfeifer, J. and Bax, A. (1995) *J. Biomol. NMR*, **6**, 277–293.

Emerson, S.D. and Montelione, G.T. (1992) *J. Magn. Reson.*, **99**, 413–420.

Gemmecker, G. and Fesik, S.W. (1991) *J. Magn. Reson.*, **95**, 208–213.

Griesinger, C., Sørensen, O.W. and Ernst, R.R. (1986) *J. Chem. Phys.*, **85**, 6837–6843.

Griesinger, C. and Eggenberger, U. (1992) *J. Magn. Reson.*, **97**, 426–434.

Karimi-Nejad, Y., Schmidt, J.M., Rüterjans, H., Schwalbe, H. and Griesinger, C. (1994) *Biochemistry*, **33**, 5481–5492.

Kleywegt, G.J., Vuister, G.W., Padilla, A., Knechtel, R.M., Boelens, R. and Kaptein, R. (1993) *J. Magn. Reson.*, **102**, 166–176.

Madsen, J.C., Sørensen, O.W., Sørensen, P. and Poulsen, F.M. (1993) *J. Biomol. NMR*, **3**, 239–244.

Montelione, G.T., Winkler, M.E., Rauenbuehler, P. and Wagner, G. (1989) *J. Magn. Reson.*, **82**, 198–204.

Pardi, A., Billeter, M. and Wüthrich, K. (1984) *J. Mol. Biol.*, **180**, 741–751.

Seip, S., Balbach, J. and Kessler, H. (1994) *J. Magn. Reson.*, **B104**, 172–179.

Shaka, A.J., Keeler, J., Frenkiel, T. and Freeman, R. (1983) *J. Magn. Reson.*, **52**, 335–338.

Sklenar, V., Piotto, M., Leppik, R. and Saudek, V. (1993) *J. Magn. Reson.*, **A102**, 241–245.

Sørensen, O.W., Eich, G.W., Levitt, M.H., Bodenhausen, G. and Ernst, R.R. (1983) *Prog. NMR Spectrosc.*, **16**, 163–192.

Tjandra, N., Grzesiek, S. and Bax, A. (1996) *J. Am. Chem. Soc.*, **118**, 6264–6272.

Tolman, J.R., Flanagan, J.M., Kennedy, M.A. and Prestegard, J.H. (1995) *Proc. Natl. Acad. Sci. USA*, **92**, 9279–9283.

Vuister, G.W. and Bax, A. (1993a) *J. Am. Chem. Soc.*, **115**, 7772–7777.

Vuister, G.W. and Bax, A. (1993b) *J. Magn. Reson.*, **B102**, 228–231.

Vuister, G.W., Yamazaki, T., Torchia, D.A. and Bax, A. (1993) *J. Biomol. NMR*, **3**, 297–306.

Wang, A.C. and Bax, A. (1995) *J. Am. Chem. Soc.*, **117**, 1810–1813.

Wang, A.C. and Bax, A. (1996) *J. Am. Chem. Soc.*, **118**, 2483–2494.

Weisemann, R., Rüterjans, H., Schwalbe, H., Schleucher, J., Bermel, W. and Griesinger, C. (1994) *J. Biomol. NMR*, **4**, 231–240.

Wider, G., Neri, D., Otting, G. and Wüthrich, K. (1989) *J. Magn. Reson.*, **85**, 426–431.

Xu, R.X., Olejniczak, E.T. and Fesik, S.W. (1992) *FEBS Lett.*, **305**, 137–143.